JOURNAL OF PROPULSION AND POWER
Vol. 26, No. 4, July–August 2010

Size Distribution of Particles in Combustion Products of Aluminized Composite Propellant

R. Jeenu,* Kiran Pinumalla,† and Desh Deepak‡
Vikram Sarabhai Space Centre, Thiruvananthapuram 695 022, India

DOI: 10.2514/1.43482

An experimental study is carried out to measure the size distribution of condensed particles in the combustion products of aluminized composite propellant using quench bomb technique. One meter long and 200 mm diameter quench bomb with propellant specimens of mass ∼32 g is used. The effects of geometry of propellant specimen, quench distance, and chamber pressure on the particle size distribution are investigated. Size distribution of the particles is measured by laser diffraction particle size analyzer and the surface structure is examined by scanning electron microscope. The study shows that the particles are spherical and their sizes vary from 0.1 to 300 μm. The particles have trimodal distribution with modes at ∼1 μm, ∼4 μm, and ∼70 μm. Although modes 1 and 4 μm particles are alumina, mode 70 μm particles are aluminum agglomerates. About 30% of aluminum present in the propellant converts into agglomerates. Results also show that coalescence of particles is higher if the particles have higher residence time in the high-temperature region or when the flow is more turbulent. From the particle size distribution obtained in the quench bomb tests, the size distribution is deduced for the combustion chamber of rocket motor.

I. Introduction

ALUMINUM powder is one of the important ingredients of most of the current composite propellants due to its high heat of combustion and density. On combustion, aluminum produces aluminum oxide (alumina) in condensed phase. These condensed particles vary in size from submicron to a few hundred microns, and have the beneficial effect of providing efficient damping of pressure oscillations in the rocket motor chamber. On the other hand, they are responsible for problems like slag accumulation, two phase flow loss, erosion of nozzle, and exhaust plume radiation. For the accurate estimation of these effects it is essential to know the particle size in the combustion products.

Combustion of aluminum particles is rather complex and different from that of other ingredients in the propellant. At the surface of the burning propellant, the binder and ammonium perchlorate (AP) decompose into gaseous products leaving behind the solid aluminum particles, which accumulate on the surface. Ignition of these particles is prevented by a thin layer of protective coating of alumina. When the accumulated material extends to the higher temperature regions of propellant flame, it leads to melting of aluminum, local breakdown of oxide coating, and ignition of particles. The molten aluminum particles coalesce to form agglomerates which detach and are convected away by the gases from the burning surface. As the temperature of the agglomerate reaches above alumina melting point, the molten alumina retracts to form alumina cap on the droplet, and an alumina particle is produced upon burn out. In addition to this, the oxidation of the aluminum vapor from the agglomerates produces very fine particles of alumina smoke. This plausible mechanism of combustion of aluminum particles is described by several authors [1–4]. It suggests that the size distribution of particles in the combustion products depends on the size of the agglomerates which is governed by the size of the parent aluminum particles and their percentage, the size of AP particles, fraction of coarse and fine AP particles, total solid loading in the propellant, chamber pressure and burning rate of the propellant [1,2,4–7].

Theoretical and empirical models are available in literature to predict the particle size of aluminum agglomerate and alumina [5,8,9]. The models provide insight into the physical processes involved in agglomeration and aluminum combustion and can calculate approximately the average size of particles for propellants with narrow band AP size distribution. However, in many cases these models are not adequate to predict the size distribution of particles, especially for propellants with wider AP size range. Hence, one has to rely on experimental techniques only.

Experimental methods have been adopted either through simulated motor chambers [6,10–17] or directly in the subscale motor chambers and in plume exhaust [18–21]. Compared with direct measurements in motor chamber or plume exhaust, simulated motor chamber tests such as quench bombs are much simpler, and provide valuable information on aluminum agglomeration, combustion, and particulate size distribution. The results from the quench bomb test are more relevant to the particle size distribution in the combustion chamber rather than in the nozzle region, because of possible breakup or coalescence of particles in the accelerated flow.

Slag is produced in the annular cavity of submerged nozzles by large particles in the combustion gases. During their travel toward the nozzle, these particles deviate from the gas flow path owing to their large momentum and accumulate as slag instead of ejecting through the nozzle. Using computational fluid dynamic techniques, this phenomenon can be simulated and the amount of slag formed in the motor can be predicted if the distribution of particle size in the combustion chamber is known.

In the present work, the quench bomb technique is used for the measurement of particle size distribution in the combustion products of aluminized composite propellant. The particle collection chamber is of stationary type and is of much bigger size compared with other studies [6,10–17]. This enables use of large propellant specimens for more accurate results. Effects of three parameters, viz., geometry of the propellant specimen, quench distance and chamber pressure are studied in detail. Based on these quench bomb tests, the size distribution of alumina/aluminum particles in the rocket motor chamber is computed.

II. Experimental Details

A. Propellant

Hydroxyl terminated polybutadiene, AP composite solid propellant containing 18% aluminum is used in the present study. Total

Received 28 January 2009; revision received 1 February 2010; accepted for publication 8 March 2010.

*Head, Performance Analysis Section.
†Engineer, Heat Transfer and Combustion Laboratories.
‡Head, Propellant Engineering Division.

Table 1 Size distribution of AP

AP size ranges, μm	Weight %
>500	1
500 – 355	7
355 – 300	14
300 – 100	30
100 – 75	7
75 – 45	16
<45	25

solid loading in the propellant is 86%. Ammonium perchlorate of wide range of particle size distribution, as given in Table 1, is used. Particle size of aluminum (volume weighted mean diameter) is 33 μm.

B. Quench Bomb

The schematic of the quench bomb is shown in Fig. 1. It is a thick-walled cylindrical steel chamber of 1 m length and 200 mm internal diameter. The top and bottom ends of the chamber are closed with flanges. The top flange is equipped with propellant specimen holder, safety relief valve, pressure transducer, and needle valve for nitrogen gas inlet and combustion gas exhaust. All the inner walls of the chamber are insulated. A tight fitting vessel made of stainless steel (SS), which contains the quench liquid, is placed inside the chamber. A mixture of water and acetone in equal volumetric proportion buffered with about 5% ammonium acetate (by weight) is used as the quench liquid. The water-acetone mixture is chosen due to its good wetting property [12]. About 3.5 liters of quench liquid is used in a test. The propellant specimen is suspended from the top flange using a SS tube. The distance of the propellant specimen from the quench liquid can be varied by using SS tubes of different lengths. A quartz plate is kept at the bottom of the SS vessel to protect the base from possible flame impingement during propellant burning. Thin nichrome wire (200 μm diameter) is used for the ignition of the propellant specimens.

C. Variation of Test Parameters

Three parameters that can affect the size distribution of particles are identified. These are geometry of the propellant specimen, quench distance, and chamber pressure.

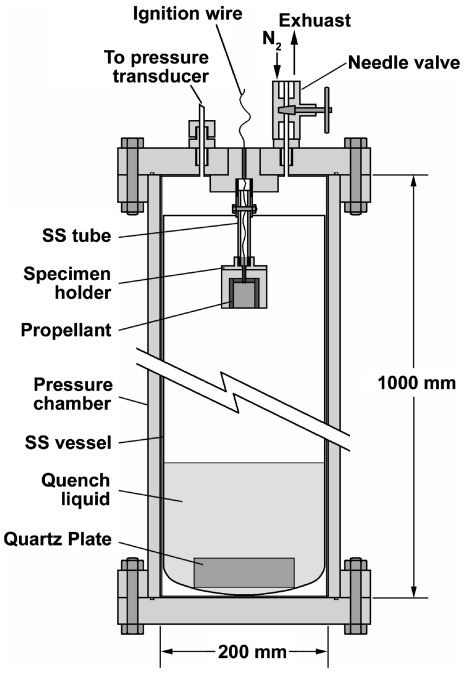

Fig. 1 The quench bomb.

1. *Specimen Geometry*

Tests are carried out with machined propellant specimens (Fig. 2) of three different geometries: 1) flat specimen (length 19 mm, diameter 35 mm), 2) short ported specimen (length 35 mm, inner diameter 25 mm, web thickness 5 mm), and 3) long ported specimen (length 70 mm, inner diameter 12 mm, web thickness 5 mm). The flat specimen is end-burning, while the other two having cylindrical ports (ported specimens) are radially burning. Dimensions of the specimens are such that the mass of all the three types of specimen is the same (~32 g). In the case of ported specimen, aftend of the specimen is closed with a disk of the same propellant of thickness 5 mm and diameter matching with the inner diameter of the specimen. The nichrome wire is inserted at the center of the propellant disk for the ignition of the specimen. For the flat specimen, the igniter wire is brought to the edge of the burning end of the specimen through the side. All the outer sides of the propellant specimen are insulated with epoxy resin of about 10 mm thickness and the specimen is bonded with the specimen holder.

2. *Quench Distance*

The distance between the propellant and the surface of quench liquid is the quench distance. The particles from the burning propellant travel this distance before being quenched in the liquid. The time for which the particles are in the hot gases above the quench liquid can affect the particle size distribution due to burning or coalescence of particles.

If the propellant specimen is too close to the quench liquid in the vessel, the liquid may be pushed sideways due to gas flow. This may result in the particles hitting the surface of quartz plate instead of being quenched in the liquid. The gas flow velocity is highest in the case of long ported specimen. For this specimen, the least quench distance and the volume of the quench liquid for proper quenching of particles are fixed based on trial tests. The closest quench distance is 420 mm (called close) for the long ported specimen with 3.5 liters of quench liquid. All the other specimens are tested at the same quench distance for the comparison. Only the flat specimen (having the lowest gas velocity) is tested additionally at the quench distance of 60 mm (called very close) after confirming that the hot gas jet does not hit the quartz plate. All the specimens are also tested at another quench distance of 740 mm (called away). The volume of quench liquid in all the tests is 3.5 liters.

3. *Chamber Pressure*

The chamber pressure increases during the test due to propellant burning. In the tests, the initial pressure is set at 1.8 MPa so that the average test pressure is ~3 MPa. To study the effect of pressure on particle size distribution, the long ported specimen is tested at a lower average pressure (~1.5 MPa) also. Tests at higher pressures could not be done due to limitation on the operating pressure of the quench bomb.

D. Test Procedure

Before the ignition of propellant specimen, the quench bomb is flushed with nitrogen to remove atmospheric oxygen and is then

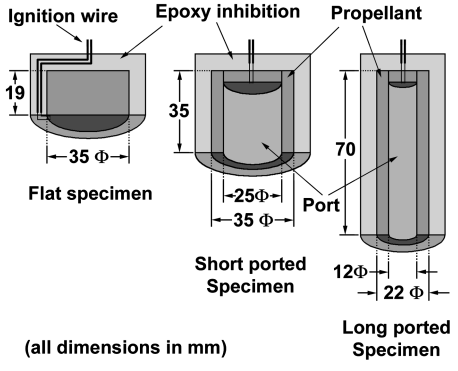

Fig. 2 Different geometries (cross section) of the propellant specimens.

Table 2 The scheme of tests

Sl. No.	Test	Specimen	Port length	Quench distance	Average pressure
1.	FVN	Flat	No port	Very close (60 mm)	Normal (∼3 MPa)
2.	FCN	Flat	No port	Close (420 mm)	Normal (∼3 MPa)
3.	FAN	Flat	No port	Away (740 mm)	Normal (∼3 MPa)
4.	SCN	Short ported	35 mm	Close (420 mm)	Normal (∼3 MPa)
5.	SAN	Short ported	35 mm	Away (740 mm)	Normal (∼3 MPa)
6.	LCN	Long ported	70 mm	Close (420 mm)	Normal (∼3 MPa)
7.	LAN	Long ported	70 mm	Away (740 mm)	Normal (∼3 MPa)
8.	LCL	Long ported	70 mm	Close (420 mm)	Low (∼1.5 MPa)

pressurized with nitrogen to the required initial test pressure (∼1.8 MPa). The pressure in the quench bomb is recorded during the test.

During the burning of the specimen, the combustion products flow downward and most of the particles get quenched in the liquid. However, a small portion of the fine particles may remain suspended in the gas above the quench liquid. To settle the suspended particles in the quench liquid, the bomb is allowed to stand still for about two hours before release of gas pressure. Computations show that two hours are sufficient for settling of all the suspended alumina particles bigger than 0.7 μm. After the slow release of pressure of the bomb, the quench liquid along with the particles (slurry) is quantitatively transferred to a glass jar. Fine particles sticking to the inner walls of the SS vessel are transferred to the glass jar by washing with buffered water-acetone mixture.

Chances of contamination of slurry with char particles from burned epoxy insulation are minimal because the specimen burning time is short (1 to 1.5 s). In the case of ported specimens, the flame reaches the insulation only at the burnout. However, in flat specimens, the flame is in contact with the insulation during propellant burning. Post-test examination of the insulation showed the insulation being intact in all the tests without much charring. In the slurry, a trace amount of carbon particles is found floating. Because the amount of these carbon particles is very small, their influence on the overall particle size distribution is neglected.

E. Measurement of Particle Size Distribution

The particle size distribution in the slurry is measured by laser diffraction particle size analyzer (Malvern Mastersizer-2000) using a small amount of representative sample from the slurry. Collection of samples from the slurry using pipette, suction syringe, sampling bottle or siphoning was not successful, because reproducible results were not obtained. Hence, a slurry sampler as shown in Fig. 3 is designed. It consists of two cups (with O-ring) made of Teflon, fixed at the ends of a pair of tongs. Using this sampler, a fixed volume of sample can be quickly withdrawn from the bulk slurry when it is being stirred mechanically. The sampler can transfer 4 ml of slurry at a time to the particle size analyzer. To disperse the particles well during the particle size measurement, the liquid in the analyzer tank is mechanically stirred and ultrasound is applied. The reproducibility of quench bomb tests is checked by repeating a few tests at the same experimental condition.

F. Separation and Analysis of Particles

The particles of size >20 μm and in the size range ∼4.5 to 20 μm are separated by sedimentation. First, ultrasound is applied to the slurry to disperse the particles and then the particles in the slurry are allowed to settle for 9 min in a long glass jar. The top portion of liquid of height 350 mm in the jar which contains particles of size <20 μm is siphoned out. This process is repeated several times to ensure complete separation. Each time, the volume of slurry is made up to the original level by adding distilled water and ultrasound is applied. The siphoned out portion of the slurry is separately allowed to settle for three hours to collect particles in the size range ∼4.5 to 20 μm. The collected particles in both the above ranges are dried in the oven. A portion of the collected particles is subjected to chemical analysis for the estimation of free aluminum.

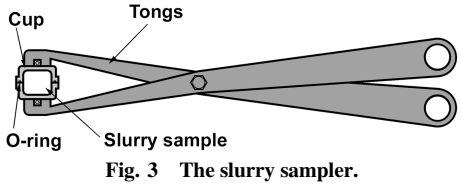

Fig. 3 The slurry sampler.

Examination of the shape and microstructure of particles is carried out using scanning electron microscope (SEM) of make Jeol, JSM 5600LV, Japan. For this, the particles are spread over an adhesive coated graphite paper stuck over the stub and a thin coating of gold is given over the particles to make them electrically conductive.

III. Results and Discussion

The scheme of quench bomb tests is given in Table 2. The results of particle size distribution and the characteristics of particles (observed by SEM) are discussed below.

A. Particle Size Distribution

The measured particle size distributions (volume percentage) in various tests are plotted in Fig. 4. The data show a deviation of ∼1 to 3% from the average value in repeated tests. This deviation may be due to small variation in representative slurry samples transferred to the particle size analyzer in repeated measurements. Figure 4 shows that the particles are in the size range 0.1 to 300 μm and the size distribution is multimodal.

To further analyze the data of each test, it is assumed that the particles with a particular mode follow the log-normal frequency distribution [22,23] and the overall size distribution of particles in a test is the sum of such log-normal distributions as given by Eq. (1):

$$\varphi(X) = [1/\sqrt{(2\pi)}]\Sigma\{(a_i/\sigma_i)\exp[-((X-\xi_i)/(\sqrt{2}\sigma_i))^2]\}$$
$$\text{and} \quad \Sigma a_i = 1 \tag{1}$$

where X is the logarithm of particle diameter, φ is the frequency function of X, ξ_i and σ_i are the average and standard deviation of the logarithm of the diameter of particles with ith mode, respectively, and a_i is the volume fraction of particles of ith mode.

Equation (1) with three modes fits well with the measured particle size distribution in most of the tests. However, four-modal distribution is required for two tests viz. FVN and SCN. The constants used for fitting the Eq. (1) are obtained by trial and are given in Table 3. The fitted distribution for each mode and the overall distribution are shown in Fig. 4. They show that, in general, most of the particles in the combustion products are distributed around three modes: ∼1 μm, ∼4 μm, and ∼70 μm. However, particles with mode at 70 μm are not present in FCN, FAN, and SAN tests (see Table 3). In FCN and FAN tests, particles are present around 34 and 13 μm, respectively. Furthermore, in FVN and SCN tests, particles are seen at modes 20 and 10 μm, respectively, in addition to the above three modes.

B. Characteristics of Mode 4 μm and 70 μm Particles

As mentioned earlier, the particles of size ranges ∼4.5 to 20 μm and >20 μm are separated by sedimentation for the examination by

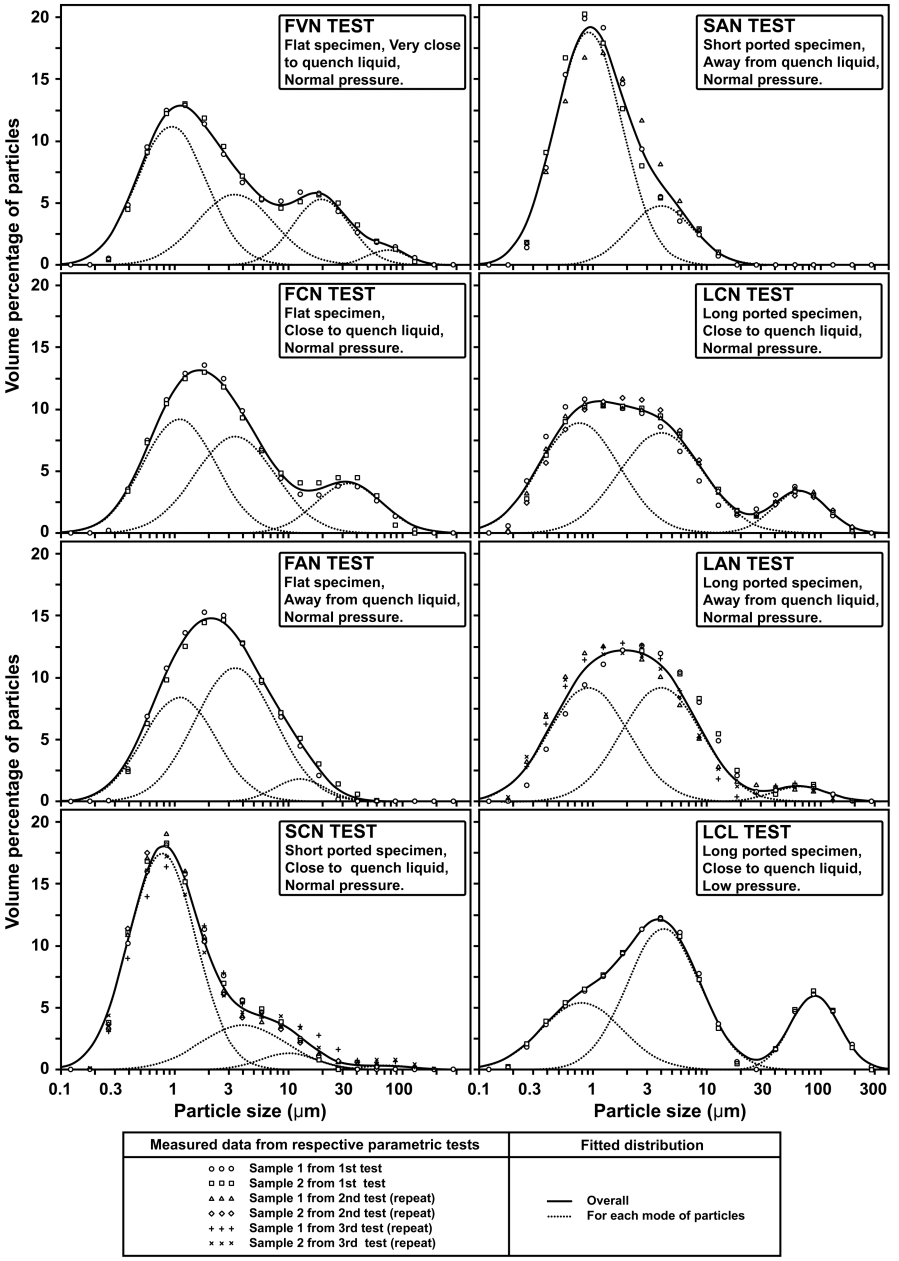

Fig. 4 Size distribution of particles in combustion products for various quench bomb tests.

SEM. Figure 4 indicates that the major part of the particles in the former range is in mode 4 μm and later range is in mode 70 μm.

Two types of particles, gray and white colored, are seen in the particles that are >20 μm separated by sedimentation. The gray particles appear bigger but are lighter than the white particles because they accumulate at the top when the container of particles is gently tapped. This helps to separate these two types of particles for the examination by SEM. The amount of white particles is very small

Table 3 Constants of Eq. (1) for fitting quench bomb test data and computing particle size distribution in motor chamber

Serial number	Test	Mode 1 μm			Mode 4 μm			Mode 70 μm			Intermediate sizes		
		10^{ξ}	a	σ	10^{ξ}	a	σ	10^{ξ}	a	σ	10^{ξ}	a	σ
		For the quench bomb test data											
1	FVN	0.9	0.50	0.31	3.4	0.28	0.34	74	0.03	0.18	20	0.19	0.25
2	FCN	1.1	0.43	0.32	3.4	0.40	0.35	——	——	——	34	0.17	0.29
3	FAN	1.1	0.39	0.32	3.4	0.55	0.35	——	——	——	13	0.06	0.22
4	SCN	0.8	0.75	0.29	4.0	0.19	0.37	71	0.01	0.24	10	0.05	0.25
5	SAN	0.9	0.80	0.29	4.0	0.20	0.28	——	——	——	——	——	——
6	LCN	0.8	0.45	0.35	4.0	0.43	0.37	66	0.12	0.24	——	——	——
7	LAN	0.9	0.48	0.35	4.0	0.48	0.35	66	0.04	0.24	——	——	——
8	LCL	0.8	0.28	0.35	4.2	0.53	0.32	89	0.19	0.21	——	——	——
		In motor chamber											
9	Near burning surface	1.0	0.58	0.32	4.0	0.15	0.35	70	0.27	0.24	——	——	——
10	Toward the nozzle-end	1.0	0.50	0.32	4.0	0.50	0.35	——	——	——	——	——	——

[a]Note: ξ and σ are in the unit of $\log_{10}$ (μm).

compared with gray particles. The color of the particles denotes that the white particles are possibly alumina, whereas the gray particles are most likely aluminum agglomerate. Chemical analysis showed that the gray particles (from an LCN test) contain ∼66% free aluminum, while no free aluminum is present in white particles or particles in the size range ∼4.5 to 20 μm.

1. *SEM of Gray Particles*

The gray particles are spherical in shape with imperfections (potholes and burrows) on the surface (Fig. 5). Some of the particles have wart-like protrusions. These particles are similar to the aluminum particles shown in [1], which experience heating and subsequent cooling in laboratory test. The surface structure of particles indicates the flow of molten material, possibly aluminum (Fig. 6). As observed by Price and Sigman [2], the potholes and burrows show that the agglomerate is not completely transformed to molten droplet before it gets quenched. The inner structure of the agglomerate shows the presence of accumulates with original aluminum particles or their oxide shells (Fig. 7). The wrinkles or dendrite-like patterns on the inner structure may be due to the contraction of the molten aluminum in the oxide shell of the particles on rapid cooling during quenching.

2. *SEM of White Particles*

SEM micrographs of the white particles are shown in Fig. 8. These particles are smaller compared with gray particles. They are spherical in shape with few or no imperfections on the surface. A broken white particle (Fig. 9) found in the sample is used to understand the internal structure of the white particles. The outer crust on the particle (of ∼10 μm thickness) is possibly formed due to rapid cooling. The inner core, which cools and solidifies later, detaches from the outer crust and cracks due to shrinkage. The outer crust is porous, while the inner core is flaky.

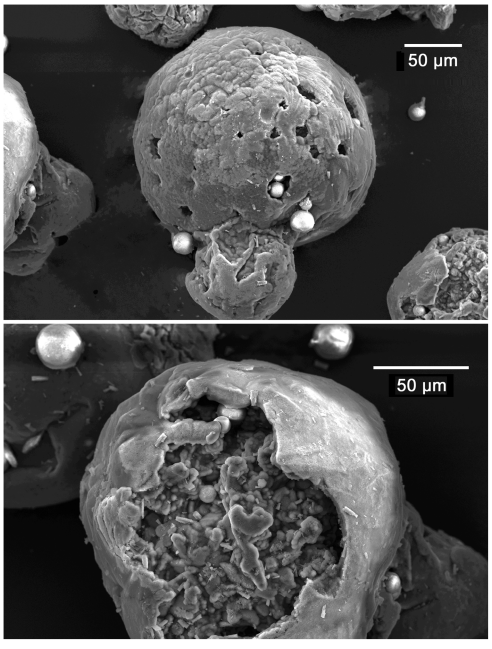

Fig. 5 The gray particles.

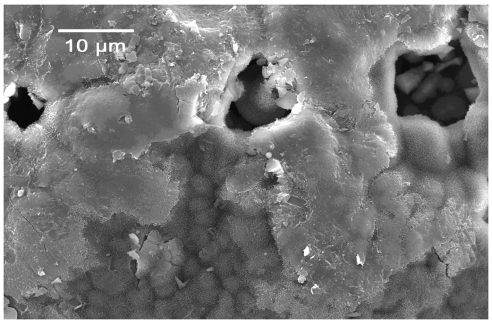

Fig. 6 Surface structure of gray particle with burrows.

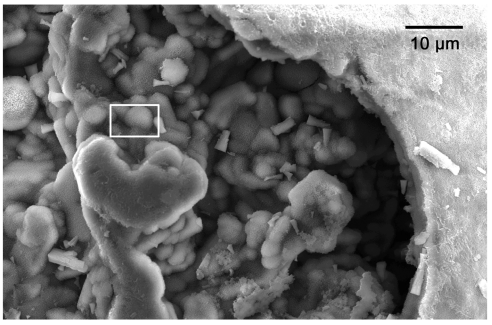

a)

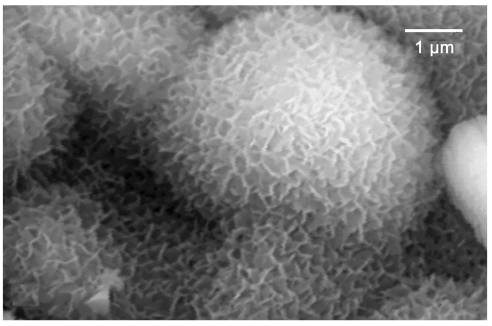

b)

Fig. 7 Internal structure of gray particle; part b is a magnified view of the portion marked in part a.

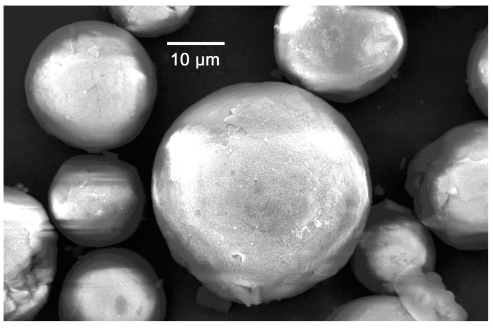

Fig. 8 The white particles.

3. *SEM of Particles in the Range of* ∼4.5 *to* 20 μm

The SEM micrograph of particles in the range ∼4.5 to 20 μm separated by sedimentation is shown in Fig. 10. Close view of the particles shows that they are spherical with smooth surface.

The mechanism of aluminum combustion in propellant described in the literature [1,3] enunciates three types of condensed particles in the combustion products: 1) smoke oxide particles (<2 μm) primarily formed by the oxidation of aluminum vapor, 2) residual oxide particles (5–50 μm) formed from the molten oxide caps on the aluminum particles or agglomerates at its burn out, whose size range is largely determined by the size of the original aluminum particles added to the propellant, thickness of the protective oxide layer on these particles, size of the agglomerate, etc., and 3) partly oxidized aluminum agglomerate particles (30 to 300 μm). These three types of particles formed through different routes can produce three distinct peaks in the particle size distribution. In the present study

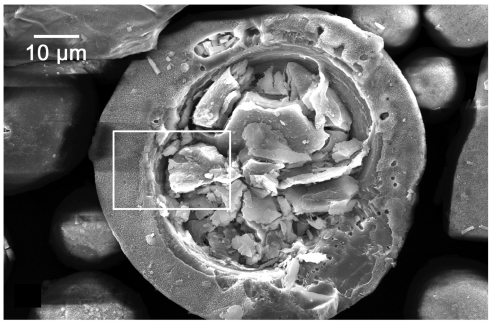

a)

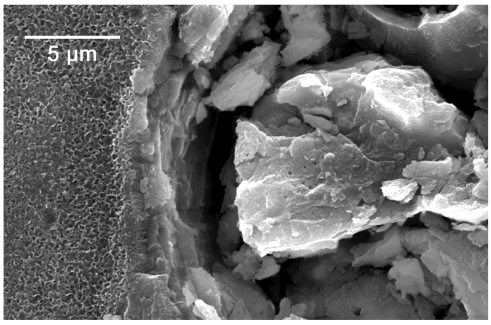

b)

Fig. 9 Internal structure of white particle; part b is a magnified view of the portion marked in part a.

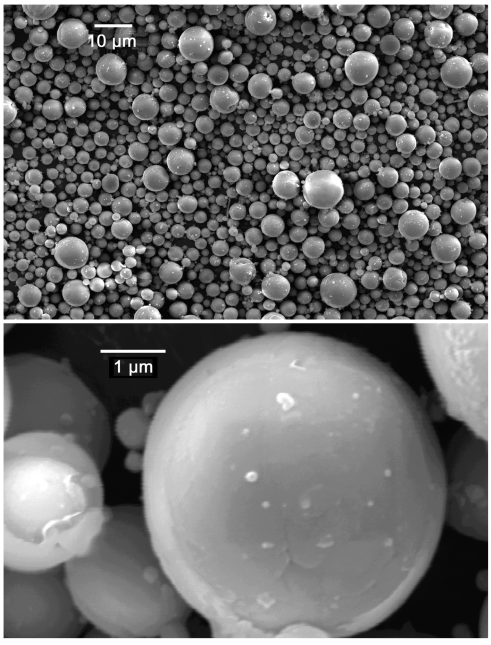

Fig. 10 Particles in the range of ~4.5 to 20 μm separated by sedimentation (overall and magnified views).

also, the size distribution of particles is trimodal with modes in the size ranges mentioned above. Thus, mode 1 μm particles could be smoke oxide particles; mode 4 μm are the residual oxide particles formed from the oxide caps, and mode 70 μm are the aluminum agglomerates. Log-normal distribution is adopted for approximate quantification of the particles in different groups.

C. Effect of Parameters on Particle Size Distribution

Figure 4 shows that the parameters, viz. specimen geometry, quench distance and pressure, do not substantially change the modes (1 μm, 4 μm, and 70 μm) but significantly affect the quantity of particles within the modes. The percentage of particles is given in Table 4, from which the following points can be deduced:

1) In all the tests, majority of the particles are with modes 1 and 4 μm. The percentage of mode 70 μm particles reduces or becomes nil with increase in quench distance.

2) For flat specimens, intermediate size particles (modes 13, 20, and 34 μm) are also present. The ratio of the percentage of mode 1 to mode 4 μm particles decreases with the increase in quench distance.

3) For the short ported specimen, the amount of mode 1 μm particles is considerably higher than the amount of mode 4 μm particles whereas they are in equal proportion for the long ported specimen. However, their ratio is independent of the quench distance for both short and long ported specimens.

4) At lower pressure, higher amount of mode 4 μm particles are formed compared with mode 1 μm particles.

5) The percentage of mode 70 μm particles is higher for long ported specimen and the percentage increases with decrease in pressure.

It is mentioned above in Sec. III.B that mode 4 μm particles could be residual oxide particles formed from the oxide cap on aluminum particles or agglomerates. In fact, an oxide coat on the surface of the original aluminum particle (33 μm) due to the oxidation of $\sim$0.2% of the aluminum can give a residual oxide particle of size $\sim$4 μm. If all the mode 4 μm particles are residual oxide particles, their number should approximately be equal to the number of aluminum particles in the propellant. Nevertheless, experimental results in Table 4 show large percentage of mode 4 μm particles (19 to 55%) in the combustion products; in terms of number of particles, this is several times higher (180 to 470 times) than the number of aluminum particles originally present in the propellant. This indicates that a considerable amount of mode 4 μm particles have been formed by the coalescence of mode 1 μm particles (smoke oxide particles). The possibility of coalescence of the smoke oxide particles is increased due to little or no net convection of gases in the outward direction from the flame envelope of aluminum particle [1].

In the experiment, the aluminum particles ejected from the burning propellant surface have to pass through varying temperature regions before quenching. Figure 11 shows the approximate distribution of temperature in the quench bomb at $\sim$3 MPa for the three types of specimens, as calculated by computational fluid dynamics. Near the burning surface of the propellant and inside the port, mixing of the hot combustion gases with the cold gases present in the quench bomb is insignificant and the gas temperature is close to the adiabatic flame temperature ($\sim$3375 K) [24]. Beyond this, the gas temperature continuously decreases due to increased mixing with cold gases. The temperature, gas velocity, and residence time of particles in these regions are plausible parameters that affect particles size distribution. For the present analysis, the temperature regions are broadly divided into two: 1) a high-temperature region (HTR) with temperature above the melting point of alumina (2328 K), where the molten alumina particles can coalesce to form bigger particles, and 2) a lower temperature region (LTR) below the melting point of alumina, where the alumina particles solidify and do not coalesce. However, it can be noted that the burning aluminum particles coming out from the HTR continue to burn in the LTR also. In the close vicinity of these burning aluminum particles in LTR, the flame temperature is high enough for the alumina particles to be in molten state and coalesce but away from the burning particle the alumina particles solidify. The residence time of particles in the different temperature regions can be obtained from the particles' velocity and length of the temperature regions. The velocity of particle is assumed equal to the gas velocity, which is computed considering the flow as a freejet and using the equations given in [25]. The HTR is assumed to be the nonmixing region of the freejet. The temperature of the nonmixing region is close to the adiabatic flame temperature, which is higher than the temperature limit chosen for the HTR. Because at the boundary of the nonmixing region, the drop in temperature is steep, the boundary of HTR can be assumed close to the boundary of the nonmixing region. In addition, because the nonmixing region is conical in shape [25], the effective length of HTR is taken as half of its total length. The gas velocities in different regions are calculated as follows:

Table 4 The volume percentage of particles in different modes

Serial number	Test	Volume percentage of particles			
		Mode 1 μm	Mode 4 μm	Mode 70 μm	Intermediate sizes
1	FVN	50	28	3	19 (20 μm)
2	FCN	43	40	——	17 (34 μm)
3	FAN	39	55	——	6 (13 μm)
4	SCN	75	19	1	5 (10 μm)
5	SAN	80	20	——	——
6	LCN	45	43	12	——
7	LAN	48	48	4	——
8	LCL	28	53	19	——

Table 5 Approximate length, average gas velocity, and residence time in different temperature regions

Serial number	Test	High-temperature region				Low-temperature region		Total residence time, ms	% of mode 70 μm particles	Ratio of mode 1 to 4 μm particles
		Length, mm	Gas velocities, m/s		Residence time, ms	Length, mm	Gas velocities, m/s			
			port	outside						
1	FVN	60	——	4.8	13	——	4.8	13	3	1.8:1
2	FCN	112	——	4.8	24	308	3.4	115	0	1.1:1
3	FAN	112	——	4.8	24	628	2.9	237	0	0.7:1
4	SCN	131	15.8	26.9	5.8	324	19.4	22	1	4:1
5	SAN	131	15.8	26.9	5.8	644	16.9	44	0	4:1
6	LCN	124	43.9	83.0	2.2	366	52.0	9	12	1:1
7	LAN	124	43.9	83.0	2.2	686	47.4	17	4	1:1
8	LCL	124	66.6	125.9	1.5	366	78.6	6	19	0.5:1

1) For the ported specimens, the gas velocity inside the port is taken as the average of the gas velocity at the aftend and at the exit of the port. The gas velocities at the aftend and at the exit of the port are calculated from the burning rate of propellant (7.4 mm/s at 3 MPa).

2) The velocity of gas in the HTR outside the port is assumed to be equal to the port exit velocity.

3) The velocity of gas between the HTR and the surface of quench liquid is taken as the average of the port exit velocity and velocity at the distance of the quench liquid surface. The length, average gas velocity, and residence time in the two regions are given in Table 5.

During the burning of propellant, aluminum ejected as single particle burns out within a short period of time. The burning time of the aluminum single particle (average size $\sim$33 μm) calculated by the equation given in [26] (in the oxidants H_2O and CO_2 formed by the combustion of the binder alone with AP [24]) is $\sim$3 ms. Therefore, the residence time of particles in HTR given in Table 5 indicates that considerable portion of the aluminum particles that do not agglomerate burns out in HTR for all the specimens. The combustion of these particles mostly produces smoke oxide particles of mode $\sim$1 μm and a portion of these particles coalesce to form bigger particles. The coalescence of the particles is higher if the flow is more turbulent [27] or the residence time of the particle in HTR is high. Thus, the probable reasons for higher amount of mode $\sim$4 μm particles in the combustion products are high flow velocity and associated increased turbulence (in the case of long ported specimen) and high residence time of particles in HTR (in the case of flat specimen).

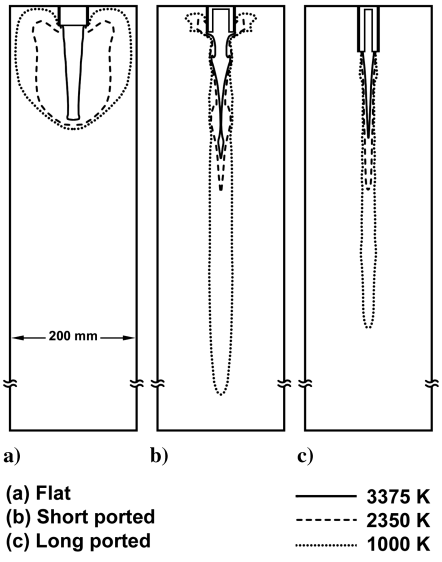

Fig. 11 Approximate distribution of temperature in the quench bomb at ~ 3 MPa for the three types of specimens obtained by computational fluid dynamics method.

The volume percentage of mode 70 μm particles (aluminum agglomerates) in various tests is also given in Table 5. Compared with aluminum single particles, these agglomerates burn for longer time due to their size and eventually get quenched in the liquid. Combustion of these particles can be represented by the equation [26,28]:

$$D^n = D_o^n - kt \tag{2}$$

where D_o is the initial diameter of the particle, D is the diameter at time t, n and k are constants. Because the volume of the particle is proportional to D^3, it can be approximated that the volume percentage of mode 70 μm particles to the power of $n/3$ is proportional to t. In Fig. 12, the percentage of mode 70 μm particles to the power of $n/3$ is plotted against the total residence time. A value of 1.8 is assumed for n [26]. Figure 12 shows that at $t = 0$ (ie., at the propellant burning surface) $\sim$25% of the total particles are of mode 70 μm. This means that $\sim$30% of aluminum in the propellant agglomerates at the propellant surface. Figure 12 also shows that almost all mode 70 μm particles will burnout within $\sim$25 ms. The burning time of 70 μm particles calculated by the equation given in [26] (in the oxidants H_2O and CO_2 formed by the combustion of the binder and nonagglomerated aluminum particles with AP [24]) is

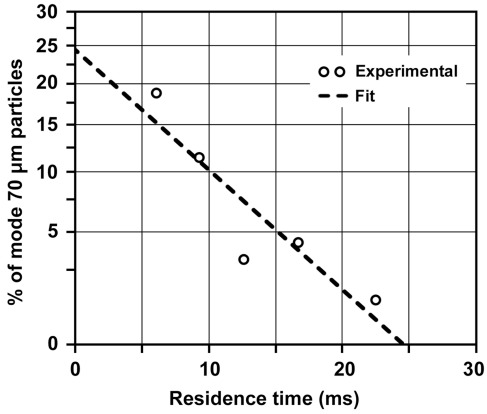

Fig. 12 Percentage of mode 70 μm particles (plotted in the power of 0.6 scale) versus total residence time.

$\sim$25 ms. Thus, the burning time of mode 70 μm particles obtained from the analysis (Fig. 12) is in line with the calculated value.

From the above analysis, it can be concluded that:

1) About 25% of the particles formed near the propellant burning surface are mode 70 μm particles (agglomerates) that will burn out completely in $\sim$25 ms.

2) Mode 4 μm (residual oxide) particles are formed not only from the alumina cap on the aluminum particles or agglomerates but also by coalescence of mode 1 μm particles. When the flow is more turbulent or the particles have high residence time in the HTR, the coalescence of particles is high.

D. Extension of Quench Bomb Results to Motor Chamber Conditions

The size distribution of particles in the motor chamber can be different from that in the quench bomb due to the differences in the thermal environment. Moreover, the two parameters in quench bomb tests viz. specimen geometry and quench distance, which significantly affect the particle size distribution, are not the parameters for combustion in the motor chamber. Hence, from these test results it is necessary to deduce a probable size distribution in the motor chamber.

The quench bomb tests showed that the particles have log-normal distribution mainly around three modes: $\sim$1 μm, $\sim$4 μm and $\sim$70 μm and their mode values do not considerably vary with pressure and other parameters such as specimen geometry or quench distance. Hence, even though the conditions in the motor are different from that of the quench bomb, the trimodal distribution with same modes as that of the quench bomb can be expected in the motor chamber. Thus, if the standard deviation and volume fraction of particles for each mode is known, the particle size distribution in the motor chamber can be calculated using Eq. (1).

Analysis of quench bomb results indicates that $\sim$25% of the total particles near the burning propellant surface are mode 70 μm particles (aluminum agglomerates). These particles continue to burn as they travel through the hot gas medium and their percentage reduces to zero in $\sim$25 ms (Fig. 12). The agglomeration of aluminum particles takes place close to the propellant surface where the thermal environment does not vary much either in the quench bomb or in the motor chamber. Therefore, it is assumed that in the motor chamber also $\sim$25% of the total particles near the propellant surface are mode 70 μm particles. The burning time of these particles in the motor chamber is also considered to be the same as that of the quench bomb tests (i.e., $\sim$25 ms) because the burning time is not a strong function of temperature of gases around the particles [25].

Present study indicates that more number of smoke oxide particles (mode 1 μm) coalesce to bigger (mode $\sim$4 μm) particles when the particles have higher residence time in the HTR or the flow is more turbulent. In large booster motors, the average residence time of particles in the chamber may be 50–200 ms and the gas velocity may reach up to 0.2–0.3 M at the nozzle-end of the grain. Thus, higher amount of mode 4 μm particles formed by the coalescence of mode 1 μm particles can be expected in the motor especially towards the nozzle-end of the grain. The long ported specimen or flat specimen (with sufficient quench distance) have burning similar to the above conditions for coalescence. In these tests, the ratio of the percentages of mode 1 to 4 μm particles is 1:1 or lower. This ratio may be further lower in the motor chamber because the residence time of particles in the chamber is quite large. On the other hand, at the head-end of the motor or near the propellant surface, as the residence time and gas velocity are low, higher quantities of mode 1 μm particles can be expected than 4 μm particle (similar to the short ported specimens). Thus, for the present computation, the ratio of $\sim$1:1 for mode 1 to 4 μm particles is assumed near the nozzle-end of the motor and the ratio of 4:1 is assumed at the head-end or near the propellant surface. The fraction of mode 70 μm particles is maximum (0.25) near the burning surface of propellant of the motor; this reduces to zero as the particles move away toward the nozzle-end.

Regarding the statistical dispersion of particle size in different quench bomb tests, large deviation of the value is not observed for a particular mode (Table 3). Therefore, an average value of σ_i for each mode is taken. In Table 3, the constants of Eq. (1) considered for the motor chamber at the propellant surface and towards the nozzle-end are also given. The particle size distributions in the motor chamber calculated using these constants are traced in Fig. 13. It indicates that the distribution varies along the port for large motors. Similarly, the particle distribution can be different for small motors and large boosters in spite of using the same propellant because the residence time of particle in the combustion chambers are different.

In the above calculation, it is assumed that the size of the particles in the motor chamber is the same as that in the quench liquid. The increased size of particles due to thermal expansion at high temperature in the motor chamber is not taken into account. For large particles, the sizes at higher temperature may be maintained in the quench liquid due to the formation of outer crust or shell over the particles on quenching. On sudden cooling, contraction of matter of the inner core leads to its detachment from the crust thus producing voids (Figs. 5 and 9). However, for small particles the size at high temperature cannot be maintained in the quench liquid. Hence, the size increase due to thermal expansion of these small particles at motor chamber temperature needs to be considered for a more realistic picture.

In the present work, the available quench bomb results are extended to predict the possible size distribution of particles in motor chamber. However, further parametric study is required to get more accurate value of the ratio of the amount of mode 1 μm to mode 4 μm particles especially close to the propellant surface. Also, quantitative information on the effect of residence time and gas velocity on the coalescence of smoke particles is necessary for better prediction. Further, in the present quench bomb test, the average test pressure is limited to $\sim$3 MPa, which is lower than the average operating pressure of many actual rocket motors. Quench bomb experiments are to be carried out at higher pressures to understand the pressure effect on the particle size distribution with more clarity. At present, no data is available to us to validate the extension of quench

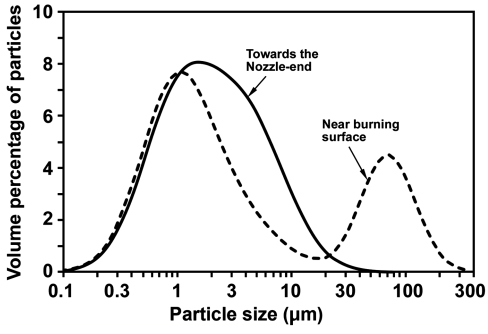

Fig. 13 Size distribution of particles in the combustion chamber of motor.

bomb results to motor chamber. Such studies have to be carried out as future work.

IV. Conclusions

Size distribution of condensed particles in the combustion products of 18% aluminized hydroxyl terminated polybutadiene–ammonium perchlorate propellant is measured using quench bomb technique. The effects of geometry of specimen, quench distance and pressure on particle size distribution are studied. The particle size is measured by laser diffraction particle size analyzer and the surface structure is examined by scanning electron microscope. The study shows that the particles are spherical and their sizes vary from 0.1 to 300 μm. In general, the particles have trimodal distribution with modes at $\sim$1 μm, $\sim$4 μm, and $\sim$70 μm. The mode 1 μm particles are smoke oxide particles formed by the burning of aluminum vapor. The mode 4 μm particles are formed from the residual oxide on aluminum particles or agglomerates at burnout and also by the coalescence of mode 1 μm particles. The study indicates that coalescence of particles is higher if the particles have higher residence time in the HTR or if the flow is more turbulent. The mode 70 μm particles are aluminum agglomerates. For the propellant used in the present study, about 30% of aluminum present in the propellant converts to aluminum agglomerates (mode 70 μm particles) which burn completely in about 25 ms. Based on the quench bomb test results, size distribution of particles in the combustion chamber of rocket motor is obtained.

Acknowledgments

The particle size analysis was carried out at the Analytical and Spectroscopic Division and the computational fluid dynamics computations were done at the Fluid Mechanics and Thermal Analysis Division of Vikram Sarabhai Space Centre. The authors are extremely thankful to M. S. Padmanabhan, former Group Director of the Propulsion Group at Vikram Sarabhai Space Centre, for helpful suggestions during the program.

References

[1] Price, E. W., "Combustion of Metalized Propellants," *Fundamentals of Solid-Propellant Combustion*, edited by Kuo, K. K., and Summerfield, M., Vol. 90, Progress in Astronautics and Aeronautics, AIAA, New York, 1984, pp. 479–513.

[2] Price, E. W., and Sigman, R. K., "Combustion of Aluminized Solid Propellants," *Solid Propellant Chemistry, Combustion, and Motor Interior Ballistic*, edited by Yang, V., Brill, T. B., and Ren, W. Z., Vol. 185, Progress in Astronautics and Aeronautics, AIAA, Virginia, 2000, pp. 663–687.

[3] Price, E. W., Comments on "Role of Aluminum in Suppressing Instability in Solid Propellant Rocket Motors," *AIAA Journal*, Vol. 9, No. 5, 1971, pp. 987–990.

[4] Fabignon, Y., Orlandi, O., Trubert, J. F., Lambert, D., and Dupays, J., "Combustion of Aluminum Particles in Solid Rocket Motors," AIAA Paper 2003-4807, July 2003.

[5] Cohen, N. S., "A Pocket Model for Aluminum Agglomeration in Composite Propellants," *AIAA Journal*, Vol. 21, No. 5, 1983, pp. 720–725.

[6] Dokhan, A., Price, E. W., Sigman, R. K., and Seitzman, J. M., "The Effects of Al Particle Size on the Burning Rate and Residual Oxide in Aluminized Propellants," AIAA Paper 2001-3581, July 2001.

[7] Babuk, V. A., Vassiliev, V. A., and Sviridov, V. V., "Formation of Condensed Combustion Products at the Burning Surface of Solid Rocket Propellant," *Solid Propellant Chemistry, Combustion, and Motor Interior Ballistic*, edited by Yang, V., Brill, T. B., and Ren, W. Z., Vol. 185, Progress in Astronautics and Aeronautics, AIAA, Virginia, 2000, pp. 749–776.

[8] Hermsen, R. W., "Aluminum Oxide Particle Size for Solid Rocket Motor Performance Prediction," *Journal of Spacecraft and Rockets*, Vol. 18, No. 6, 1981, pp. 483–490.

[9] Jackson, T. L., Najjar, F., and Buckmaster, J., "New Aluminum Agglomeration Models and Their Use in Solid-Propellant-Rocket Simulations," *Journal of Propulsion and Power*, Vol. 21, No. 5, 2005, pp. 925–936.

[10] Sambamurthi, J. K., Price, E. W., and Sigman, R. K., "Aluminum Agglomeration in Solid-Propellant Combustion," AIAA Journal, Vol. 22, No. 8, 1984, pp. 1132–1138.

[11] Braithwaite, P. C., Christensen, W. N., and Daugherty, V., "Quench Bomb Investigation of Aluminum Oxide Formation from Solid Rocket Propellants, Part I: Experimental Methodology," *25th JANNAF Combustion Meeting*, Chemical Propulsion Information Agency, Vol. 1, Oct. 1998.

[12] Salita, M., "Quench Bomb Investigation of Al_2O_3 Formation from Solid Rocket Propellants, Part II: Analysis of Data," *25th JANNAF Combustion Meeting*,Chemical Propulsion Information Agency, Vol. 1, Oct. 1998.

[13] Brennan, M., "Recent Combustion Bomb Testing of RSRM Propellant," AIAA Paper 96-3270, July 1996.

[14] Liu, T. K., Perng, H. C., Luh, S. P., and Liu, F., "Aluminum Agglomeration in Ammonium Perchlorate/Cyclotrimethylene Trinitramine/Aluminum/Hydroxy—Terminated Polybutadiene Propellant Combustion," *Journal of Propulsion and Power*, Vol. 8, No. 6, 1992, pp. 1177–1184.

[15] Hardt, B. E., and Brewster, M. Q., "Investigation of Al and Mg/Al Alloy Behavior in Composite Solid Propellant Combustion," *25th JANNAF Combustion Meeting*, Chemical Propulsion Information Agency, Vol. 1, Oct. 1998.

[16] Liu, T. K., and Hsieh, C. F., "Analysis of Agglomerate Size from Burning Aluminized AP/RDX/HTPB Propellants in Quench Bomb," *Journal of Propulsion and Power*, Vol. 12, No. 5, 1996, pp. 995–998.

[17] Habu, H., and Shimada, T., "Study on Al/Al_2O_3 Agglomeration Particle Size Distributions for Solid Propellants," AIAA Paper 2006-5249, July 2006.

[18] Brennan, W. D., Hovland, D. L., and Netzer, D. W., "Measured Particulate Behavior in a Subscale Solid Propellant Rocket Motor," *Journal of Propulsion and Power*, Vol. 8, No. 5, 1992, pp. 954–960.

[19] Sambamurthi, J. K., "Al_2O_3 Collection and Sizing from Solid Rocket Motor Plumes," *Journal of Propulsion and Power*, Vol. 12, No. 3, 1996, pp. 598–604.

[20] Dobbins, R. A., and Strand, L. D., "A Comparison of Tow Methods of Measuring Particle Size of Al_2O_3 Produced by a Small Rocket Motor," *AIAA Journal*, Vol. 8, No. 9, 1970, pp. 1544–1550.

[21] Youngborg, E. D., Pruitt, T. E., Smith, M. J., and Netzer, D. W., "Light-Diffraction Particle Size Measurements in Small Solid-Propellant Rockets," *Journal of Propulsion and Power*, Vol. 6, No. 3, 1990, pp. 243–249.

[22] Irani, R. R., and Callis, C. F., *Particle size: Measurement, Interpretation, and Application*, John Wiley & Sons, Inc., New York, 1963, Chaps. 3 and 4.

[23] Salita, M., "Deficiencies and Requirements in Modeling of Slag Generation in Solid Rocket Motors," *Journal of Propulsion and Power*, Vol. 11, No. 1, 1995, pp. 10–22.

[24] Gordon, S., and McBride, B. J., "Computer Program for Calculation of Complex Chemical Equilibrium Compositions, Rocket Performance, Incident and Reflected Shocks, and Chapman-Jouguet Detonations," NASA SP 273, Interim Revision, Scientific and Technical Information Office, National Aeronautics and Space Administration, Washington, D. C., March 1976.

[25] Tilton, J. N., "Fluid and Particle Dynamics," *Perry's Chemical Engineers' Handbook*, 8th ed., edited by Perry, R. H., and Green, D. W., McGraw–Hill, New York, 1997, pp. 6-20–6-21.

[26] Beckstead, M. W., "A Summary of Aluminum Combustion," *RTO/VKI Special Course on Internal Aerodynamics in Solid Rocket Propulsion*, The Applied Vehicle Technology Panel and the Von Kármán Institute for Fluid Dynamics, Rhode-Saint-Genèse, Belgium, Jan. 2004.

[27] Wang, L. P., Xue, Y., Ayala, O., and Grabowski, W. W., "Effects of Stochastic Coalescence and Air Turbulence on the Size Distribution of Cloud Droplets," *Atmospheric Research*, Vol. 82, Nos. 1–2, Nov. 2006, pp. 416–432.

[28] Melcher, J. C., Krier, H., and Burton, R. L., "Burning Aluminum Particles Inside a Laboratory-Scale Solid Rocket Motor," *Journal of Propulsion and Power*, Vol. 18, No. 3, 2002, pp. 631–640.

S. Son
Associate Editor